Published in final edited form as:
Nature. 2007 December 20; 450(7173): 1195–1200. doi:10.1038/nature06416.

Locally dynamic synaptic learning rules in pyramidal neuron dendrites

Christopher D. Harvey[1,2] and **Karel Svoboda**[1,2]

[1]Janelia Farm Research Campus, HHMI, Ashburn, VA 20147

[2]Watson School of Biological Sciences, Cold Spring Harbor Laboratory, Cold Spring Harbor, NY 11724

Abstract

Long-term potentation (LTP) of synaptic transmission underlies aspects of learning and memory. LTP is input-specific at the level of individual synapses, but neural network models predict interactions between plasticity at nearby synapses. Here we show in hippocampal pyramidal cells that LTP at individual synapses reduces the threshold for potentiation at neighboring synapses. Following input-specific LTP induction by two-photon glutamate uncaging or synaptic stimulation, subthreshold stimuli, which by themselves were too weak to trigger LTP, now caused robust LTP and spine enlargement at neighboring spines. Furthermore, LTP induction broadened the presynaptic-postsynaptic spike interval for spike-timing-dependent LTP within a dendritic neighborhood. The reduction in LTP induction threshold lasted ~ 10 minutes and spread over ~ 10 micrometers of dendrite. These local interactions between neighboring synapses support clustered plasticity models of memory storage and could allow for the binding of behaviorally-linked information on the same dendritic branch.

Long-lasting modifications of synaptic strength (long-term potentiation, LTP) are critical for learning and memory in many parts of the brain, including the hippocampus[1]. The extent to which LTP is synapse-specific influences a neuron's information processesing and storage. LTP can be input-specific[2], even at the level of individual synapses[3], indicating that synapses may function as independent units of plasticity[4]. However, neighboring synapses might be co-regulated due to the heterosynaptic spread of LTP over short stretches of dendrite[5].

Neural network models predict interactions between plasticity at nearby synapses. Heterosynaptic metaplasticity suggests that LTP at one set of synapses may subsequently increase the threshold for potentiation at other synapses[6, 7]. In contrast, clustered plasticity models[8-10] predict a decrease in the threshold for LTP in the neighborhood of recently potentiated synapses, for example due to local synaptic tagging[10-12]. To distinguish between these possibilities, we probed the coupling between plasticity at nearby synapses using two-photon glutamate uncaging[3, 13-16] combined with two-photon laser scanning microscopy[17, 18] and perforated patch whole-cell recordings of synaptic currents.

Crosstalk between plasticity at nearby synapses

Does LTP at one synapse influence the threshold for plasticity at neighboring synapses? We looked for such 'crosstalk' in acute hippocampal slices from GFP-expressing transgenic mice[19]. Dendritic spines were imaged on proximal (distance to the soma < 100 μm)

Correspondence: K.S. (svobodak@janelia.hhmi.org).

secondary and tertiary apical dendrites of CA1 pyramidal neurons (Fig 1a,c,e). Glutamate receptors on individual spines were stimulated with two-photon glutamate uncaging and the resulting excitatory postsynaptic currents (uEPSCs) were measured at the soma using perforated patch clamp recordings.

To induce LTP at individual spines we paired a train of 30 stimuli (0.5 Hz) with postsynaptic depolarization to ~ 0 mV[3]. In this 'LTP protocol' each uncaging stimulus (4 ms duration) triggered NMDA-R-mediated spine $[Ca^{2+}]$ accumulations that were similar to $[Ca^{2+}]$ transients evoked by low-frequency synaptic stimulation at 0 mV[20] or by tetanic stimulation[21] (Supplementary Fig 1b-c, see Supplementary information). $[Ca^{2+}]$ accumulations were restricted to the stimulated spine (Supplementary Fig 1a-c), indicating that glutamate did not spread to activate neighboring spines. As a read-out of plasticity we monitored spine volumes and uEPSCs in response to test stimuli at the spine receiving the LTP protocol (LTP spine) and neighboring spines less than 4 μm from the LTP spine on the same branch. The LTP protocol resulted in a long-lasting (> 40 minutes) increase in uEPSC amplitude and spine volume at the LTP spine, but not at nearby spines ($\Delta uEPSC_{LTP\ spine}$ = 99 ± 17 %, $p < 0.01$; $\Delta uEPSC_{nearby\ spine}$ = − 1 ± 9 %, $p > 0.9$; $\Delta vol_{LTP\ spine}$ = 78 ± 10 %, $p < 0.01$; $\Delta vol_{nearby\ spines}$ = 0 ± 4 %, $p > 0.9$) (Fig 1a-b). A similar protocol, but with the amplitudes of NMDA-R-mediated spine $[Ca^{2+}]$ transients reduced by a factor of four (subthreshold protocol, 1 ms pulse duration) (Supplementary Fig 1b-c), did not change uEPSC amplitude or spine volume at the spine receiving the uncaging stimuli (sub spine) or at nearby spines ($\Delta uEPSC_{sub\ spine}$ = − 1 ± 2 %, $p > 0.4$; $\Delta uEPSC_{nearby\ spine}$ = 2 ± 2 %, $p > 0.6$; $\Delta vol_{sub\ spine}$ = 1 ± 1 %, $p > 0.6$; $\Delta vol_{nearby\ spines}$ = 1 ± 4 %, $p > 0.8$) (Fig 1c-d).

To test for crosstalk, we induced LTP at one spine (LTP spine) and, 90 seconds later, provided the subthreshold protocol at a neighboring spine (sub spine). The subthreshold protocol now triggered LTP and a long-lasting spine enlargement ($\Delta uEPSC_{LTP\ spine}$ = 95 ± 11 %, $p < 0.01$; $\Delta uEPSC_{sub\ spine}$ = 97 ± 10 %, $p < 0.01$; $\Delta vol_{LTP\ spine}$ = 76 ± 16 %, $p < 0.02$; $\Delta vol_{sub\ spine}$ = 81 ± 10 %, $p < 0.01$) (Fig 1e-f). The levels of functional and structural plasticity were similar in spines receiving the LTP and subthreshold protocols (uEPSC: $p > 0.5$; Vol: $p > 0.5$) (Fig 1g). Other nearby spines that received neither stimulus did not change (Δvol = 1 ± 1 %, $p > 0.7$). Crosstalk did not occur following application of the LTP protocol at a postsynaptic potential of ~ −70 mV, which did not induce LTP, arguing that crosstalk is triggered by LTP induction and not by the uncaging process itself (see Supplementary information). LTP induction at one spine therefore lowered the threshold for potentiation at nearby spines, while maintaining input specificity.

The changes in uEPSC amplitude and spine volume were highly correlated[3, 22] ($r = 0.86$, $p < 0.0001$) (Fig 1h), consistent with documented relationships between spine volume, postsynaptic density (PSD) area, and the number of AMPA receptors in the PSD[14, 23, 24]. These observations confirm that spine enlargement is a structural correlate of LTP[3, 22].

Crosstalk in unperturbed neurons

The pairing LTP protocol (Fig 1) has non-physiological features. For example, depolarization of the postsynaptic neuron during pairing causes global Ca^{2+} influx through voltage-gated calcium channels (VGCCs), which could contribute to the crosstalk between synapses. To test if crosstalk occurs without sustained postsynaptic depolarization, we stimulated NMDA-Rs on individual spines from unperturbed neurons (in nominally 0 mM Mg^{2+}). Uncaging stimuli triggered $[Ca^{2+}]$ transients that were restricted to the activated spine (Supplementary Fig 1a-c). Each uncaging pulse during the LTP protocol produced NMDA-R currents (7.9 ± 1.1 pA; Supplementary Fig 1a,d) that corresponded to the opening of ~ 5 NMDA-Rs, comparable to the number of receptors opened by low frequency synaptic

stimulation[25]. The LTP protocol triggered a large transient increase in spine volume in the LTP spine that decayed to a persistent spine enlargement after 10 minutes; spines neighboring the stimulated spine did not change (ΔvolLTP spine = 76 ± 18 %, $p < 0.01$; $\Delta vol_{nearby\ spines} = -1 \pm 4$ %, $p > 0.7$) (Fig 2b,e,f). The subthreshold protocol, which produced ~ 4-fold lower NMDA-R currents and [Ca^{2+}] accumulations (Supplementary Fig 1a-d), triggered only transient changes in spine volume that decayed within 10 minutes (Δvolsub spine = 5 ± 6 %, $p > 0.3$) (Fig 2c,e,f). We next provided the LTP protocol at one spine and, 90 seconds later, tested for crosstalk by applying the subthreshold protocol at a neighboring spine. The subthreshold protocol now induced sustained spine enlargement of the same size as the LTP protocol (Δvol_{LTP} spine = 66 ± 8 %, $p < 0.0001$; Δvolsub spine = 67 ± 10 %, $p < 0.0001$; LTP spine vs. sub spine: $p > 0.95$) (Fig 2d-f). Other spines that received neither stimulus did not change (Δvol = 0 ± 1 %, $p > 0.95$). Similar results were obtained in cultured rat hippocampal slices (Supplementary Fig 2a-d). Persistent postsynaptic depolarization therefore was not required to observe the crosstalk in plasticity between synapses.

Crosstalk with synaptically-induced plasticity

Glutamate released by uncaging may activate a distinct set of receptors compared to synaptically-released glutamate. We therefore tested if crosstalk occurs following synaptically-induced plasticity. Schaffer collateral axons were stimulated (120 pulses, 2 Hz) in low extracellular Mg^{2+} [3, 26]. This 'synaptic LTP protocol' induced long-lasting spine enlargement in a sparse subset of spines (see Methods). The magnitude of the spine volume change ($\Delta vol_{synaptic\ LTP\ spine} = 70 \pm 14$ %, $p < 0.001$) was similar to that triggered by the uncaging LTP protocol[3] ($p > 0.8$; cf Fig 3e and Fig 2b). Spine enlargement was thus used to identify synapses potentiated by synaptic stimulation (see Methods). To test for crosstalk, we provided the subthreshold protocol at a nearby spine (sub spine) two minutes after the synaptic LTP protocol. The subthreshold protocol, which by itself did not trigger structural plasticity (Fig 2c,e,f), now induced a persistent spine enlargement (Δvolsub spine = 62 ± 9 %, $p < 0.001$) of similar magnitude to the synaptically-induced volume change ($p > 0.6$) (Fig 3b-e). Other nearby spines did not change (Δvolnearby spines = −3 ± 5 %, $p > 0.4$) (Fig 3b-e). Synaptically-induced plasticity therefore reduced the threshold for potentiation at neighboring synapses.

Modulation of the window for spike-timing-dependent LTP

Excitatory postsynaptic potentials (EPSPs) followed by action potentials (APs) within a short time window (tens of milliseconds) can trigger LTP[27]. The magnitude of this spike-timing-dependent potentiation (STDP) decreases monotonically with the time between the EPSP and the AP[28, 29]. Because crosstalk reduces the threshold for potentiation in the neighborhood of the LTP spine, crosstalk could broaden the spike time window (Δt) for STDP at neighboring spines. We induced STDP with uncaging pulses (60 pulses, 2 Hz) followed (Δt = 5 ms) by three APs at 50 Hz. The amplitudes of uEPSPs (0.41 ± 0.19 mV, mean ± sd) were similar to those of miniature EPSPs[30]. This induction protocol induced long-lasting increases in the uEPSC amplitude and spine volume at the stimulated spine, but not at nearby spines within 4 μm on the same dendritic branch ($\Delta uEPSC_{\Delta t = 5\ ms} = 62 \pm 17$ %, $p < 0.02$; $\Delta uEPSC_{nearby\ spine} = 5 \pm 8$ %, $p > 0.5$; $\Delta vol_{\Delta t = 5\ ms} = 57 \pm 13$ %, $p < 0.01$; $\Delta vol_{nearby\ spines} = 0 \pm 3$ %, $p > 0.8$) (Fig 4b,d). The magnitudes of functional and structural plasticity decreased as the time between the uEPSP and the APs increased ($\tau_{\Delta uEPSC} = 17.6$ ms, $\tau_{\Delta vol} = 16.6$ ms) (Fig 4c). Pairing at longer intervals (Δt = 35 ms) did not trigger LTP or spine enlargement ($\Delta uEPSC_{\Delta t = 35\ ms} = -3 \pm 10$ %, $p > 0.8$; $\Delta vol_{\Delta t = 35\ ms} = 4 \pm 3$ %, $p > 0.2$) (Fig 4e), indicating that uEPSPs or APs alone were not sufficient to trigger LTP. STDP therefore was induced at single spines in an input-specific manner.

We next induced STDP at one spine with an uEPSP-AP time window of 5 ms and, 90 seconds later, stimulated a neighboring spine with an uEPSP-AP interval of 35 ms. Under these conditions, the uEPSP-AP pairing at the 35 ms time window now induced LTP and a long-lasting spine enlargement ($\Delta uEPSC_{\Delta}t$ = 5 ms = 67 ± 10 %, $p < 0.01$; $\Delta uEPSC_{\Delta}t$ = 35 ms = 69 ± 8 %, $p < 0.01$; $\Delta vol_{\Delta}t$ = 5 ms = 68 ± 9 %, $p < 0.01$; $\Delta vol_{\Delta}t$ = 35 ms = 74 ± 15 %, $p < 0.02$) (Fig 4f). The levels of functional and structural plasticity were similar in spines receiving the pairing at short and long intervals (uEPSC: $p > 0.4$; vol: $p > 0.4$) (Fig 4g), and the changes in uEPSC amplitude and spine volume were highly correlated ($r = 0.81$, $p < 0.0001$) (Fig 4h). Other nearby spines that received neither stimulus did not change (Δvol = −1 ± 1 %, $p > 0.7$). LTP induction at one spine therefore broadened the uEPSP-AP time window for STDP at neighboring spines.

Characterization of crosstalk

We next measured the time scale of the crosstalk in plasticity between synapses. We varied the time between the LTP and subthreshold protocols given in low extracellular Mg^{2+}, while maintaining the distance between the stimulated spines at ~ 3 μm. The crosstalk was measured as the volume change triggered by the subthreshold protocol at the sub spine following LTP induction at the LTP spine. Crosstalk decreased gradually with time and lasted up to 10 minutes ($t_{1/2}$ = 5.3 minutes) (Fig. 5a).

To determine the length scale of the crosstalk we varied the distance between the spines receiving the LTP and subthreshold protocols, while keeping the time between stimuli at 90 seconds. Crosstalk decreased gradually with distance for up to ~ 8 μm in both directions along the parent dendrite (full-width at half maximum = 11.1 μm) (Fig 5b). The magnitude of crosstalk was similar for spines farther or closer to the apical trunk with respect to the spine receiving the LTP protocol (data not shown). The length scale of the crosstalk was similar in cultured rat hippocampal slices (full-width at half maximum = 10.2 μm) (Supplementary Fig 2e). Consistently, when spines separated by ~ 10 μm were stimulated by the LTP and subthreshold protocols paired with depolarization to ~ 0 mV, the subthreshold protocol did not induce functional or structural plasticity ($\Delta uEPSC_{sub\ spine}$ = −7 ± 5 %, $p > 0.15$; $\Delta vol_{sub\ spine}$ = −8 ± 8 %, $p > 0.4$) (Fig 5c). Furthermore, following synaptically-induced spine enlargement, the subthreshold protocol did not trigger structural plasticity at spines located ~ 10 μm from the enlarged spine ($\Delta vol_{sub\ spine}$ = −3 ± 8 %, $p > 0.9$) (Fig 5d).

Our experiments suggest that LTP induction activates a factor at the LTP spine that spreads to reduce the threshold for potentiation at neighboring synapses. Extracellular diffusible factors have been implicated in the heterosynaptic spread of LTP[31, 32]. Similarly, intracellular factors can spread over the relevant time and length scales[33, 34] (unpublished observations). To distinguish between extracellular and intracellular factors we examined whether crosstalk can occur between spines that are close within the neuropil (< 4 μm), but are located on different dendritic branches and thus far in terms of cytoplasmic distance (> 50 μm). We induced LTP at one spine and, 90 seconds later, provided the subthreshold protocol at the sub spine less than 4 μm away on a nearby dendritic branch from the same cell. Under these conditions, the subthreshold protocol failed to induce structural plasticity ($\Delta vol_{sub\ spine}$ = 1 ± 9 %, $p > 0.6$) (Fig 6a), indicating that intracellular factors, rather than extracellular factors, were necessary for the crosstalk between synapses.

Ca^{2+} release from intracellular stores has been implicated in the heterosynaptic spread of some forms of synaptic plasticity[35, 36]. However, eliminating Ca^{2+} release from intracellular stores using thapisgargin (1 μM) and ryanodine (20 μM) (Supplementary Fig 3) did not affect the crosstalk between synapses ($\Delta vol_{sub\ spine}$ = 67 ± 19 %, $p > 0.95$) (Fig 6b).

The crosstalk in plasticity between neighboring synapses described here shares characteristics with synaptic tagging, in which early LTP at one set of synapses can be converted into late LTP by the strong stimulation of a second group of synapses[11]. Synaptic tagging-based plasticity occurs both when the 'weak' stimulus precedes and follows the 'strong' stimulus[37, 38]. We therefore tested if the crosstalk in plasticity depends on the order of stimuli. When the subthreshold protocol preceded the LTP protocol by 90 seconds, the subthreshold protocol did not induce spine enlargement (Δvolsub spine = 2 ± 14 %, $p > 0.8$) (Fig 5a). Because synaptic tagging-based crosstalk requires the capture of newly synthesized proteins[11, 39], we also tested the role of protein synthesis in the crosstalk between neighboring synapses. Application of the protein synthesis inhibitor anisomycin (25 μM) had no effect on the spine enlargement induced by the LTP and subthreshold protocols (ΔvolLTP spine = 63 ± 11 %, $p > 0.7$; Δvolsub spine = 79 ± 17 %, $p > 0.3$) (Fig 6b). Similar results were obtained with other protein synthesis inhibitors (60 μM cycloheximide, Δvolsub spine = 64 ± 16 %, $p > 0.9$ and 50 μM emetine, Δvolsub spine = 78 ± 8 %, $p > 0.6$). As a positive control for inhibitor function, anisomycin, cycloheximide, and emetine caused a rapid decrease in destabilized EGFP fluorescence[40] (Supplementary Fig 4). The crosstalk in plasticity between neighboring spines is therefore distinct from synaptic tagging.

Discussion

We have shown that the induction of plasticity at individual synapses can be influenced by events at neighboring synapses. LTP induction at one synapse decreased the threshold for potentiation at nearby synapses within ~ 10 μm for ~ 10 minutes. Crosstalk did not perturb input-specificity per se, and therefore differed from the heterosynaptic spread of plasticity[5, 31, 32, 35]. However, the reduction in LTP induction threshold in the vicinity of a potentiated synapse may help explain discrepancies between data showing the heterosynaptic spread of LTP[5] and synapse-specific LTP at single spines[3]. Previous studies have suggested that synaptic plasticity can be influenced by prior neural activity[6, 7, 11, 12, 41-43]. However, the time courses of these interactions were much longer compared to the time scale of crosstalk reported here. Furthermore, these studies did not establish a length scale for crosstalk.

What cellular mechanisms could underlie the crosstalk in plasticity between neighboring synapses? Our results suggest that the intersynaptic spread of intracellular signaling factors likely plays a key role. The time scale and spatial scale of crosstalk are consistent with a diffusing cytoplasmic factor[33, 34] (unpublished observations). This factor could modify synaptic properties at nearby spines to decrease the threshold for LTP or may provide enzymatic activity that is necessary for LTP induction but is not produced by subthreshold stimuli.

Although synaptic modifications can occur in an input specific manner[3] (Fig 1a-b, Fig 2b, Fig 4d), the coordinated regulation of groups of 10-20 synapses within a dendritic neighborhood indicates that individual synapses do not necessarily function as independent units of plasticity. Models of clustered plasticity[8-10] propose that individual engrams could be stored in synapses sharing the same dendritic branch, which would increase the information storage capacity of the neuron through the non-linear summation of synaptic inputs[8, 9, 30, 44]. Clustered plasticity implies the binding of inputs that are active during the same behavioral epochs on the same dendritic branch. It will be of interest to map the distribution of the information carried by synapses within the dendritic trees of individual neurons.

Methods

Preparation

Acute hippocampal brain slices (300 μm thick) from Thy1 GFP mice[19] (line M; postnatal day 14-18) were prepared in accordance with the animal care and use guidelines of Cold Spring Harbor Laboratory and Janelia Farm Research Campus. Slices were cut in gassed (95% O_2 / 5% CO_2), ice-cold cutting solution containing (in mM) 110 choline chloride, 25 $NaHCO_3$, 25 D-glucose, 2.5 KCl, 7 $MgCl_2$, 0.5 $CaCl_2$, 1.25 NaH_2PO_4, 11.5 sodium ascorbate, and 3 sodium pyruvate. Slices were then incubated in gassed artificial cerebral spinal fluid (ACSF) containing (in mM) 127 NaCl, 25 $NaHCO_3$, 25 D-glucose, 2.5 KCl, 1 $MgCl_2$, 2 $CaCl_2$, and 1.25 NaH_2PO_4 at 35°C for 30 minutes and then at room temperature until used. Experiments were performed at room temperature except for those in Fig 3 (33° C). MNI-caged-L-glutamate, CPP, NBQX, thapsigargin, and ryanodine were from Tocris; amphotericin B was from Sigma; and, TTX, anisomycin, emetine, and cycloheximide were from Calbiochem.

Electrophysiology

Perforated patch clamp recordings were used to prevent the washout of intracellular signaling molecules and LTP[28, 46]. The internal solution contained 136.5 mM potassium gluconate, 17.5 mM KCl, 9 mM NaCl, 1 mM $MgCl_2$, 10 mM HEPES, 0.2 mM EGTA, and 0.5 mg/mL amphotericin B. Pipettes were front-filled with a small volume of internal solution without amphotericin. Perforations reached a stable series resistance (36 ± 8 MΩ, mean ± sd) within 30-45 minutes of seal formation. Series resistances were stable (± 20%) throughout the experiment. uEPSCs were measured in response to test stimuli (0.05 Hz) at −70 mV. uEPSC amplitudes were measured as the difference between the mean current amplitude over a 5 ms window around the peak and the mean current amplitude over a 100 ms window before the uncaging stimulus. Each time point is the average of 5 trials (Fig 1b,d,f and Fig 4d-f). Spike-timing-dependent LTP (Fig 4) was induced in current clamp mode. Action potentials were triggered by brief current injections at the soma (2 ms, 1-3 nA). Voltage clamp whole-cell recordings for [Ca^{2+}] imaging (Supplementary Fig 1) were made using an internal solution containing (in mM) 135 $CsMeSO_3$, 10 HEPES, 10 Na-phosphocreatine, 4 $MgCl_2$, 4 Na_2-ATP, 0.4 Na-GTP, 3 ascorbate, 0.03 Alexa 594, 0.5 Fluo-4FF.

Synaptic stimulation (Fig 3) was performed using short current pulses (0.1 ms, 30 μA) delivered with a glass pipette (~ 2-3 μm tip) filled with ACSF and 10 μM Alexa 594 to aid pipette placement. The pipette was positioned 10 to 20 μm from a GFP-labeled dendrite of interest. Each pulse produced an EPSP of 7.8 ± 2.7 mV (n = 7 stimulus positions from 3 cells, mean ± sd, measured in parallel experiments), corresponding to the activation of ~ 30 synapses, a small subset of the synapses on typical CA1 pyramidal cells (total ~ 10^4 synapses). Synapses activated by electrical stimulation are distributed throughout the dendritic tree, rarely with multiple activated synapses on a short stretch of dendrite[47, 48]. We identified activated synapses that had undergone plasticity based on spine enlargement. Image stacks containing a 30 μm long stretch of dendrite were compared before and immediately following the synaptic LTP protocol (120 stimuli at 2 Hz, low extracellular Mg^{2+}). ΔF/F images (Fig 3b) were generated following low-pass filtering and image alignment using cross-correlation analysis allowing for distortions. Spontaneous fluctuations in fluorescence intensity (i.e. spine volume) in non-stimulated spines had a coefficient of variation (CV) of 0.21 ± 0.02. Following the synaptic LTP protocol, spines that enlarged by more than 3 times the CV of spontaneous fluctuations (Δvol > 60%) were scored as synaptic LTP spines. Structural plasticity after synaptic stimulation was sparse, consistent with the expected activation of a small subset of synapses. 16 of 114 imaged dendrites contained at

least one enlarged spine (range 1-2 spines). For 14 of these 16 dendrites, only a single spine in the field of view enlarged following synaptic stimulation. In the two cases where multiple spines enlarged, the spine receiving the subthreshold protocol was less than 12 μm from one, but not the other, enlarged spine.

Imaging and glutamate uncaging

We used a custom-built two-photon microscope controlled by ScanImage[49]. Two Ti:sapphire lasers (910 nm for imaging GFP and 720 nm for uncaging; MaiTai, Spectra Physics) were combined with polarized optics and passed through the same set of scan mirrors and objective (see Supplementary methods). The intensity of each beam was controlled independently with electro-optical modulators (Pockels cells; Conoptics). The epifluorescence and transfluorescence signals were summed[50].

For glutamate uncaging 2.5 mM MNI-caged-L-glutamate was added to the ACSF. The laser beams were parked ~ 0.5 μm from the tip of the spine head in the direction away from the parent dendrite. For test pulses 45 mW laser power was delivered to the back focal aperture of the objective for 1 ms. During stimulus trains we used 20 mW pulses lasting 4 ms for the LTP protocol and 1 ms for the subthreshold protocol. For spike-timing-dependent LTP, all uncaging pulses were 1 ms in duration with 45 mW laser power at the back focal aperture of the objective. Approximately 20% of this laser power was transmitted through the objective. Only spines well separated from both the dendrite and neighboring spines were selected for experiments. Initial spine volumes were indistinguishable across conditions (data not shown). The distances between spines tested for uEPSC changes were similar on average (Fig 1: LTP protocol only, 3.1 ± 0.4 μm; subthreshold protocol only, 2.6 ± 0.6 μm; crosstalk, 3.5 ± 0.2 μm; ANOVA $p > 0.7$. Fig 3: $\Delta t = 5$ ms: 2.2 ± 0.3 μm; $\Delta t = 35$ ms: 2.3 ± 0.4 μm; crosstalk: 2.3 ± 0.2 μm; ANOVA $p > 0.95$). The depth in the slice was restricted to 25-50 μm.

Plasticity was induced using four protocols: (1) depolarization to ~ 0 mV in perforated patch clamp mode paired with 30 uncaging pulses at 0.5 Hz in 2 mM Ca^{2+}, 1 mM Mg^{2+}, and 1 μM TTX (Fig 1); (2) 30 uncaging pulses at 0.5 Hz in 4 mM Ca^{2+}, 0 mM Mg^{2+}, and 1 μM TTX (Fig 2); (3) 120 synaptic stimuli at 2 Hz in 4 mM Ca^{2+}, 0 mM Mg^{2+} at 33° (Fig 3); and, (4) an uncaging pulse followed by 3 APs at 50 Hz, repeated 60 times at 2 Hz in 2 mM Ca^{2+} and 1 mM Mg^{2+} in perforated patch clamp mode (Fig 4). The time window (Δt) for spike-timing-dependent LTP was defined as the time between the uncaging pulse and the first AP.

[Ca^{2+}] imaging was performed as described[48]. Images were acquired every 64 ms in frame-scan mode. [Ca^{2+}] transients were measured as the change in Ca^{2+}-sensitive green fluorescence (500 μM Fluo-4FF; ΔG) divided by the Ca^{2+}-insensitive red fluorescence (30 μM Alexa 594; R), normalized to $(G/R)_{max}$ measured in 10 mM Ca^{2+}.

Data analysis

Spine volumes were measured as the integrated green fluorescence after background subtraction, which is proportional to spine volume[45], normalized to the fluorescence intensity of the thick apical dendrite[25]. The origin of all time axes corresponds to the start of the uncaging protocols. Volume changes at nearby spines (Figs 1-4) were averaged across all neighboring spines less than 4 μm from the LTP or sub spines. uEPSC changes at nearby spines (Figs 1, 4) were from an individual neighboring spine for each experiment. In the bar graphs, Δvolume and ΔuEPSC were normalized to the baseline and measured starting 15 minutes post-stimulus until the end of the time course.

All data are presented as mean ± sem unless noted otherwise. n indicates the number of spines analyzed. One experiment was performed per cell, except to map the spike-timing-dependent LTP time window for which up to 3 experiments per cell were performed sequentially. Each figure summarizes all experiments, except for Fig 3, in which only experiments with a scored synaptic LTP spine in the field-of-view were analyzed.

p values are from two-tailed t-tests unless noted otherwise. For all t-tests the null hypothesis stated that the mean was equal to zero, except for pharmacology experiments in which the null hypothesis stated that the means of control and drug conditions were the same.

Supplementary Material

Refer to Web version on PubMed Central for supplementary material.

Acknowledgments

We thank Haining Zhong and Ryohei Yasuda for helpful discussions, Tim O'Connor for programming assistance, Kuan Hong Wang for destabilized EGFP DNA and Roberto Malinow and Jeff Magee for comments on the manuscript. This work was supported by HHMI, NIH, and a David and Fanny Luke Fellowship (CDH).

References

1. Malenka RC, Bear MF. LTP and LTD: an embarrassment of riches. Neuron. 2004; 44:5–21. [PubMed: 15450156]
2. Andersen P, Sundberg SH, Sveen O, Wigstrom H. Specific long-lasting potentiation of synaptic transmission in hippocampal slices. Nature. 1977; 266:736–737. [PubMed: 195210]
3. Matsuzaki M, Honkura N, Ellis-Davies GC, Kasai H. Structural basis of long-term potentiation in single dendritic spines. Nature. 2004; 429:761–766. [PubMed: 15190253]
4. Yuste R, Denk W. Dendritic spines as basic functional units of neuronal integration. Nature. 1995; 375:682–684. [PubMed: 7791901]
5. Engert F, Bonhoeffer T. Synapse specificity of long-term potentiation breaks down at short distances. Nature. 1997; 388:279–284. [PubMed: 9230437]
6. Abraham WC, Mason-Parker SE, Bear MF, Webb S, Tate WP. Heterosynaptic metaplasticity in the hippocampus in vivo: a BCM-like modifiable threshold for LTP. Proc Natl Acad Sci U S A. 2001; 98:10924–10929. [PubMed: 11517323]
7. Wang H, Wagner JJ. Priming-induced shift in synaptic plasticity in the rat hippocampus. J Neurophysiol. 1999; 82:2024–2028. [PubMed: 10515995]
8. Poirazi P, Mel BW. Impact of active dendrites and structural plasticity on the memory capacity of neural tissue. Neuron. 2001; 29:779–796. [PubMed: 11301036]
9. Mehta MR. Cooperative LTP can map memory sequences on dendritic branches. Trends Neurosci. 2004; 27:69–72. [PubMed: 15106650]
10. Govindarajan A, Kelleher RJ, Tonegawa S. A clustered plasticity model of long-term memory engrams. Nat Rev Neurosci. 2006; 7:575–583. [PubMed: 16791146]
11. Frey U, Morris RG. Synaptic tagging and long-term potentiation. Nature. 1997; 385:533–536. [PubMed: 9020359]
12. Martin KC, et al. Synapse-specific, long-term facilitation of aplysia sensory to motor synapses: a function for local protein synthesis in memory storage. Cell. 1997; 91:927–938. [PubMed: 9428516]
13. Furuta T, et al. Brominated 7-hydroxycoumarin-4-ylmethyls: photolabile protecting groups with biologically useful cross-sections for two photon photolysis. Proc Natl Acad Sci U S A. 1999; 96:1193–1200. [PubMed: 9990000]
14. Matsuzaki M, et al. Dendritic spine geometry is critical for AMPA receptor expression in hippocampal CA1 pyramidal neurons. Nat Neurosci. 2001; 4:1086–1092. [PubMed: 11687814]

15. Carter AG, Sabatini BL. State-dependent calcium signaling in dendritic spines of striatal medium spiny neurons. Neuron. 2004; 44:483–493. [PubMed: 15504328]
16. Sobczyk A, Scheuss V, Svoboda K. NMDA receptor subunit-dependent [Ca2+] signaling in individual hippocampal dendritic spines. J. Neurosci. 2005; 25:6037–6046. [PubMed: 15987933]
17. Denk W, Strickler JH, Webb WW. Two-photon laser scanning microscopy. Science. 1990; 248:73–76. [PubMed: 2321027]
18. Svoboda K, Yasuda R. Principles of two-photon excitation microscopy and its applications to neuroscience. Neuron. 2006; 50:823–839. [PubMed: 16772166]
19. Feng G, et al. Imaging neuronal subsets in transgenic mice expressing multiple spectral variants of GFP. Neuron. 2000; 28:41–51. [PubMed: 11086982]
20. Sabatini BS, Oertner TG, Svoboda K. The life-cycle of Ca^{2+} ions in spines. Neuron. 2002; 33:439–452. [PubMed: 11832230]
21. Muller W, Connor JA. Dendritic spines as individual neuronal compartments for synaptic Ca^{2+} responses. Nature. 1991; 354:73–76. [PubMed: 1682815]
22. Kopec CD, Li B, Wei W, Boehm J, Malinow R. Glutamate receptor exocytosis and spine enlargement during chemically induced long-term potentiation. J Neurosci. 2006; 26:2000–2009. [PubMed: 16481433]
23. Nusser Z, et al. Cell type and pathway dependence of synaptic AMPA receptor number and variability in the hippocampus. Neuron. 1998; 21:545–559. [PubMed: 9768841]
24. Takumi Y, Ramirez-Leon V, Laake P, Rinvik E, Ottersen OP. Different modes of expression of AMPA and NMDA receptors in hippocampal synapses. Nat Neurosci. 1999; 2:618–624. [PubMed: 10409387]
25. Nimchinsky EA, Yasuda R, Oertner TG, Svoboda K. The number of glutamate receptors opened by synaptic stimulation in single hippocampal spines. J Neurosci. 2004; 24:2054–2064. [PubMed: 14985448]
26. Lang C, et al. Transient expansion of synaptically connected dendritic spines upon induction of hippocampal long-term potentiation. Proc Natl Acad Sci U S A. 2004; 101:16665–16670. [PubMed: 15542587]
27. Dan Y, Poo MM. Spike timing-dependent plasticity of neural circuits. Neuron. 2004; 44:23–30. [PubMed: 15450157]
28. Bi GQ, Poo MM. Synaptic modifications in cultured hippocampal neurons: dependence on spike timing, synaptic strength, and postsynaptic cell type. J Neurosci. 1998; 18:10464–10472. [PubMed: 9852584]
29. Wittenberg GM, Wang SS. Malleability of spike-timing-dependent plasticity at the CA3-CA1 synapse. J Neurosci. 2006; 26:6610–6617. [PubMed: 16775149]
30. Losonczy A, Magee JC. Integrative Properties of Radial Oblique Dendrites in Hippocampal CA1 Pyramidal Neurons. Neuron. 2006; 50:291–307. [PubMed: 16630839]
31. Scanziani M, Malenka RC, Nicoll RA. Role of intercellular interactions in heterosynaptic long-term depression. Nature. 1996; 380:446–450. [PubMed: 8602244]
32. Schuman EM, Madison DV. A requirement for the intercellular messenger nitric oxide in long-term potentiation. Science. 1991; 254:1503–1506. [PubMed: 1720572]
33. Gray NW, Weimer RM, Bureau I, Svoboda K. Rapid Redistribution of Synaptic PSD-95 in the Neocortex In Vivo. PLoS Biol. 2006; 4
34. Tsuriel S, et al. Local sharing as a predominant determinant of synaptic matrix molecular dynamics. PLoS Biol. 2006; 4:e271. [PubMed: 16903782]
35. Nishiyama M, Hong K, Mikoshiba K, Poo MM, Kato K. Calcium stores regulate the polarity and input specificity of synaptic modification. Nature. 2000; 408:584–588. [PubMed: 11117745]
36. Royer S, Pare D. Conservation of total synaptic weight through balanced synaptic depression and potentiation. Nature. 2003; 422:518–522. [PubMed: 12673250]
37. Frey U, Morris RG. Weak before strong: dissociating synaptic tagging and plasticity-factor accounts of late-LTP. Neuropharmacology. 1998; 37:545–552. [PubMed: 9704995]

38. Casadio A, et al. A transient, neuron-wide form of CREB-mediated long-term facilitation can be stabilized at specific synapses by local protein synthesis. Cell. 1999; 99:221–237. [PubMed: 10535740]

39. Fonseca R, Nagerl UV, Morris RG, Bonhoeffer T. Competing for memory: hippocampal LTP under regimes of reduced protein synthesis. Neuron. 2004; 44:1011–1020. [PubMed: 15603743]

40. Li X, et al. Generation of destabilized green fluorescent protein as a transcription reporter. J Biol Chem. 1998; 273:34970–34975. [PubMed: 9857028]

41. Abraham WC, Bear MF. Metaplasticity: the plasticity of synaptic plasticity. Trends Neurosci. 1996; 19:126–130. [PubMed: 8658594]

42. Turrigiano GG, Nelson SB. Homeostatic plasticity in the developing nervous system. Nat Rev Neurosci. 2004; 5:97–107. [PubMed: 14735113]

43. Huang YY, Colino A, Selig DK, Malenka RC. The influence of prior synaptic activity on the induction of long-term potentiation. Science. 1992; 255:730–733. [PubMed: 1346729]

44. Golding NL, Staff NP, Spruston N. Dendritic spikes as a mechanism for cooperative long-term potentiation. Nature. 2002; 418:326–331. [PubMed: 12124625]

45. Holtmaat AJ, et al. Transient and persistent dendritic spines in the neocortex in vivo. Neuron. 2005; 45:279–291. [PubMed: 15664179]

46. Yasuda R, et al. Supersensitive Ras activation in dendrites and spines revealed by two-photon fluorescence lifetime imaging. Nat Neurosci. 2006; 9:283–291. [PubMed: 16429133]

47. Oertner TG, Sabatini BS, Nimchinsky EA, Svoboda K. Facilitation at single synapses probed with optical quantal analysis. Nat. Neurosci. 2002; 5:657–664. [PubMed: 12055631]

48. Yasuda R, et al. Imaging calcium concentration dynamics in small neuronal compartments. Sci STKE. 2004; 2004:pl5. [PubMed: 14872098]

49. Pologruto TA, Sabatini BL, Svoboda K. ScanImage: Flexible software for operating laser-scanning microscopes. BioMedical Engineering OnLine. 2003; 2:13. [PubMed: 12801419]

50. Mainen ZF, et al. Two-photon imaging in living brain slices. Methods. 1999; 18:231–239. [PubMed: 10356355]

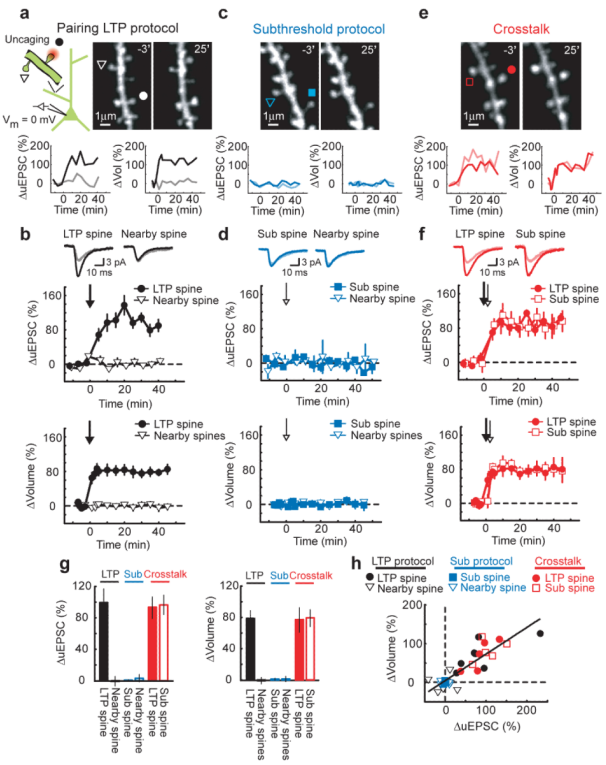

Figure 1.

Crosstalk with pairing-induced LTP

(a) Upper panel: (Left) Schematic of the experiment. (Right) Images before (−3′) and after (25′) LTP induction. At time = 0 the LTP protocol (30 uncaging pulses at 0.5 Hz, 4 ms pulse duration, postsynaptic potential 0 mV) was applied to the spine marked by a circle (LTP spine). A triangle marks a tested nearby spine. Lower panels: Changes in uEPSC amplitude and spine volume at the LTP (black) and nearby (gray) spines.

(b) Upper panels: uEPSCs, averaged across all cells, in response to test stimuli before (−3′; gray) and after (40′; black) the LTP protocol. Lower panels: Time-course of the changes in uEPSC amplitude and spine volume at the LTP (n = 7) and nearby spines (uEPSC: n = 7, Vol: n = 31). The arrow marks the LTP protocol.

(c-d) Same as for (a-b) except with the subthreshold protocol. At time = 0 the subthreshold protocol (30 uncaging pulses at 0.5 Hz, 1 ms pulse duration, postsynaptic potential 0 mV) was applied to the spine marked by a square (sub spine; n = 5). Triangles indicate nearby spines (uEPSC: n = 5, Vol: n = 26).

(e-f) Same as for (a-b) except for the crosstalk case. At time = 0 the LTP protocol was applied to the spine marked by a circle (LTP spine) and, 90 seconds later, the subthreshold protocol was given at the spine marked by a square (sub spine). n = 5, mean ± sem

(g) Changes in uEPSC amplitude and spine volume. Error bars indicate mean ± sem.

(h) Correlation between changes in uEPSC amplitude and spine volume. r = 0.86, p < 0.0001

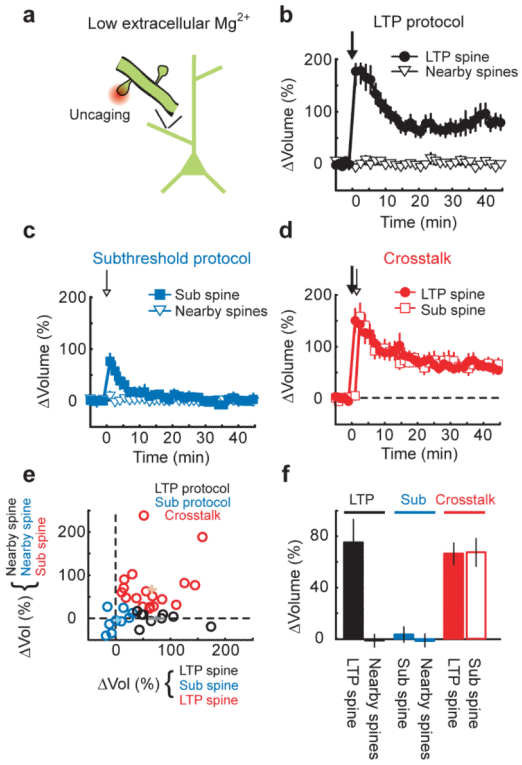

Figure 2.

Crosstalk in unperturbed neurons

(a) Schematic of the experiment.

(b) Time-course of the spine volume changes induced by the LTP protocol (applied at time = 0, 30 uncaging pulses at 0.5 Hz, 4 ms pulse duration, in low extracellular Mg^{2+}) for the stimulated (LTP spine; n = 9) and nearby spines (n = 29).

(c) Time-course of the spine volume changes induced by the subthreshold protocol (applied at time = 0, 30 uncaging pulses at 0.5 Hz, 1 ms pulse duration, in low extracellular Mg^{2+}) for the stimulated (sub spine; n = 8) and nearby spines (n = 38).

(d) Time-course of the spine volume changes for the crosstalk case. At time = 0 the LTP protocol was applied to the LTP spine and, 90 seconds later, the subthreshold protocol was given at a neighboring spine (sub spine). n = 18, mean ± sem

(e) Spine volume changes from individual experiments. Crosses indicate mean ± sem.

(f) Changes in spine volume. Error bars indicate mean ± sem.

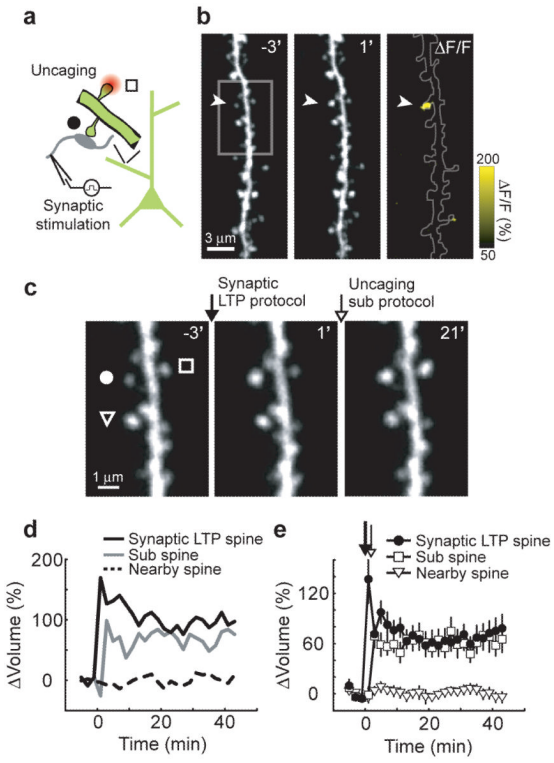

Figure 3.

Crosstalk with synaptically-induced plasticity

(a) Schematic of the experiment.

(b) Images before (−3′) and after (1′) the synaptic LTP protocol (applied at time = 0; 120 stimuli, 2 Hz in low extracellular Mg^{2+}). The arrowhead marks an enlarged spine (synaptic LTP spine). A ratio image (ΔF/F) comparing fluorescence intensity before (−3′) and after (1′) the synaptic LTP protocol is shown.

(c) High zoom images before (−3′) stimulation, after (1′) the synaptic LTP protocol (applied at time = 0), and after (21′) the subthreshold protocol (applied at time = 2 minutes). A circle, square, and triangle mark the synaptic LTP spine, the sub spine, and a nearby spine, respectively.

(d) Changes in spine volume for the example shown in (b-c).

(e) Time-course of the change in spine volume for synaptic LTP spines (n = 11), sub spines (n = 11), and nearby spines (n = 34), mean ± sem.

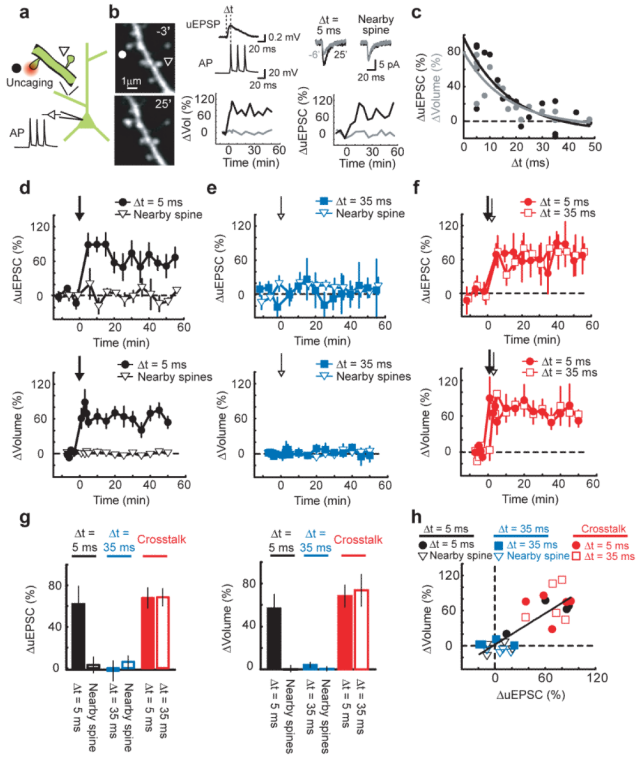

Figure 4.

Crosstalk with spike-timing-dependent LTP

(a) Schematic of the experiment.

(b) Left: Images before (−3′) and after (25′) spike-timing-dependent LTP induction. At time = 0 uncaging pulses (60 pulses at 2 Hz) followed by three APs at 50 Hz (Δt = 5 ms) were applied to the spine marked by the circle. The triangle marks a tested nearby spine. Top middle: Example uEPSPs and APs from unpaired stimuli. Top right: uEPSCs averaged over 5 trials before (−6′) and after (25′) uEPSP-AP pairing. Bottom middle, right: Changes in uEPSC amplitude and spine volume at the stimulated (black) and nearby (gray) spines.

(c) Changes in uEPSC amplitude (black) and spine volume (gray) at different uEPSP-AP time windows (Δt). Changes were measured from 20 to 30 minutes post-stimulus. Exponential fits are shown.

(d) Time-course of the changes in uEPSC amplitude and spine volume for uEPSP-AP pairing at Δt = 5 ms (n = 4) and at nearby spines (uEPSC: n = 4, Vol: n = 20). The arrow marks the time of uEPSP-AP pairing.

(e) Time-course of the changes in uEPSC amplitude and spine volume for uEPSP-AP pairing at Δt = 35 ms (n = 4) and at nearby spines (uEPSC: n = 4, Vol: n = 21).

(f) Time course of the changes in uEPSC amplitude and spine volume for the crosstalk case. At time = 0 one spine was stimulated with uEPSP-AP pairing at Δt = 5 ms and, 90 seconds later, a neighboring spine was stimulated with uEPSP-AP pairing at Δt = 35 ms. n = 5, mean ± sem.

(g) Changes in uEPSC amplitude and spine volume. Error bars indicate mean ± sem.

(h) Correlation between changes in uEPSC amplitude and spine volume. r = 0.81, p < 0.0001.

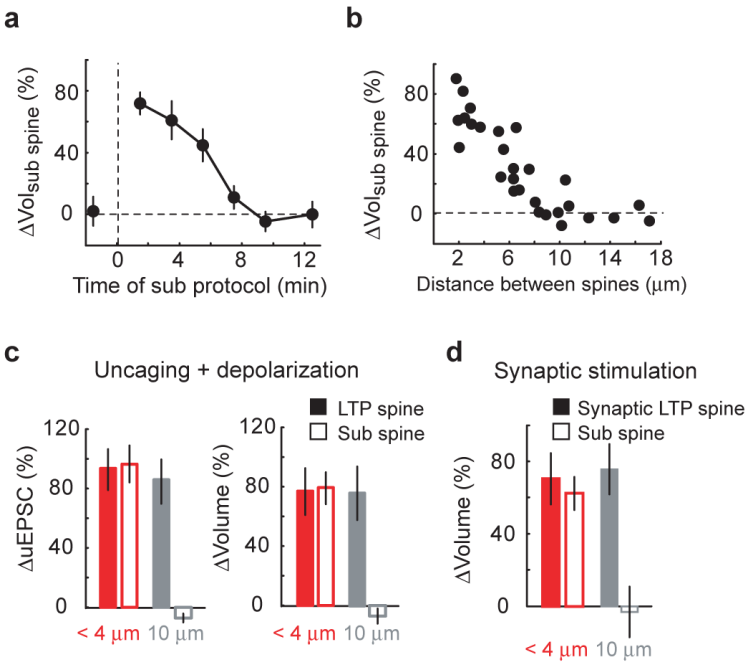

Figure 5.

Spatial and temporal scales of crosstalk

(a) Time scale of crosstalk. At time = 0, the LTP protocol was applied to a single spine (in low extracellular Mg^{2+}, see Fig 2). The subthreshold protocol was applied to a neighboring spine (sub spine) ~ 3 μm away. n ≥ 4 for all time points, mean ± sem

(b) Length scale of crosstalk. The LTP protocol was applied to a single spine and, 90 seconds later, a nearby spine (sub spine) was stimulated with the subthreshold protocol (in low extracellular Mg^{2+}, see Fig 2).

(c) Distance-dependence of crosstalk with pairing-induced plasticity. The LTP protocol (at postsynaptic potential 0 mV) was applied to the LTP spine and, 90 seconds later, the subthreshold protocol (at postsynaptic potential 0 mV) was applied to a spine (sub spine) either less than 4 μm or ~ 10 μm away (see Fig 1). The data for spines separated by less than 4 μm are from Fig 1. n = 4 at 10 μm, mean ± sem (d) Distance-dependence of crosstalk with synaptically-induced plasticity. The synaptic LTP protocol was applied in low extracellular Mg^{2+} to induce plasticity in the synaptic LTP spine. Two minutes later, the subthreshold protocol was applied to a spine (sub spine) either less than 4 μm or ~ 10 μm away (see Fig 3). The data for spines separated by less than 4 μm are from Fig 3. n = 5 at 10 μm, mean ± sem

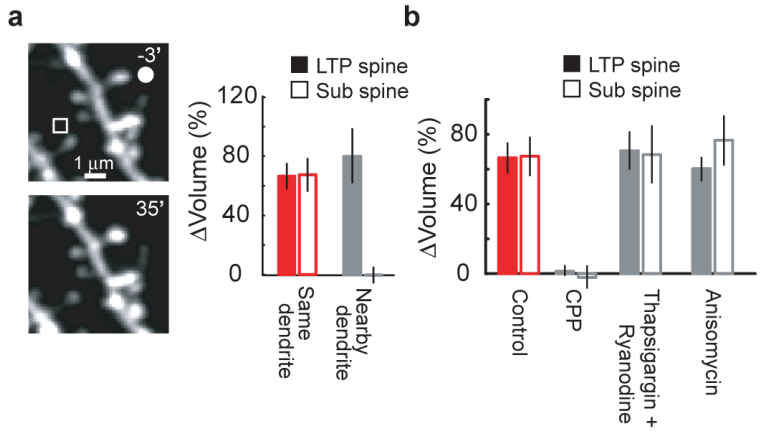

Figure 6.

Signaling underlying crosstalk

(a) Crosstalk examined at nearby dendritic branches. The LTP protocol was applied to the spine marked by a circle (LTP spine) and, 90 seconds later, the subthreshold protocol was given at a spine on a nearby dendritic branch from the same cell (sub spine, square; in low extracelluar Mg^{2+}, see Fig 2). Example images are shown. The “same dendrite” data are from Fig 2. n = 5 for nearby dendrites, mean ± sem

(b) Pharmacological analysis of crosstalk. In the presence of the specified drugs, the LTP protocol was applied to the LTP spine and, 90 seconds later, a neighboring spine (sub spine) was stimulated with the subthreshold protocol (in low extracellular Mg^{2+}, see Fig 2). Control data are from Fig 2. n = 4 each for CPP (10 μM), thapsigargin (1 μM) + ryanodine (20 μM), and anisomycin (25 μM), mean ± sem.